

¹ Drought indices of water demand and supply, soil moisture, vegetation, and
² its impact on LULCC in continental Chile

³ Francisco Zambrano^{a,1,*}

^a Universidad Mayor, Hémera Centro de Observación de la Tierra, Facultad de Ciencias, Escuela de Ingeniería en Medio Ambiente y Sustentabilidad, Santiago, Chile, 7500994

⁴ **Abstract**

Human-induced greenhouse gas emissions have increased the frequency and/or intensity of weather and climate extremes. Central Chile has been affected by a persistent drought which is impacting the hydrological system and vegetation development. The region has been the focus of research studies due to the diminishing water supply, this persistent period of water scarcity has been defined as a “mega drought”. Nevertheless, our results evidence that the water deficit has expanded beyond. Our goal is to analyze the impact of drought, measured by drought indices of water supply/demand and vegetation status, in the LULCC (land use land cover change) over continental Chile. For the analysis, continental Chile was divided into five zones according to a latitudinal gradient: “Norte Grande”, “Norte Chico”, “Zona Central”, “Zona Sur”, and “Zona Austral”. We used monthly climatic re-analysis variables for precipitation, temperature and soil moisture for 1981-2023 from ERA5-Land (ERA5L); and MODIS (Moderate-Resolution Imaging Spectroradiometer) product MCD12Q1 for land cover for 2001-2021, and the NDVI vegetation index from product MOD13A2 collection 6.1 for 2000-2023, both from collection 6.1. We estimated atmospheric evaporative demand (AED) by combining the Hargreaves-Samani equation with the ERA5L temperature. We derived the drought indices SPI (Standardized Precipitation Index), SPEI (Standardized Precipitation Evapotranspiration Index), EDDI (Evaporative Demand Drought Index), SSI (standardized anomaly of cumulative soil moisture), and the zcNDVI (standardized anomaly of cumulative NDVI). These indices were calculated for time scales of 1, 3, 6, 12, 24, and 36 months, except for zcNDVI (1, 3, and 6 months). We analyzed the temporal correlation of SPI, SPEI, EDDI, and SSI with zcNDVI to have insights into the impact of water supply and demand on vegetation. Our results showed that LULCC had an increasing trend of 412 [km²yr⁻¹] of forest expansion in the “Zona Sur”, together with a decreasing trend of 24 [km²yr⁻¹] of cropland contraction in the “Zona Central” meanwhile the “Zona Sur” showed an increase of 31 [km²yr⁻¹], and a contraction of 80 [km²yr⁻¹] of bare soil in the “Zona Austral”. The EDDI was the less correlated index for the five macro zones and the five types of land cover, showing that the temperature in Chile has little impact on vegetation. Higher r-squared values, between 0.5 and 0.8, were obtained at “Norte Chico” and “Zona Central” for the land cover types of savanna, shrubland, grassland, and croplands for the indices SPEI and SSI at time scales of 12 and 24 months. The forest type reaches a r-squared of ~0.5 for SSI of 12 months. The results indicate that the “Norte Chico” and “Zona Central” are the most sensitive regions to water supply deficits longer than a year, potentially explained by a low capacity of water storage in those zones that should be further investigated.

⁵ **Keywords:** drought, land cover change, satellite

*Corresponding author

Email address: francisco.zambrano@umayor.cl (Francisco Zambrano)

¹This is the first author footnote.

6 **1. Introduction**

7 The sixth assessment report (AR6) of the IPCC [1] indicates that human-induced greenhouse gas emissions
8 have increased the frequency and/or intensity of some weather and climate extremes, and the evidence has
9 been strengthened since AR5 [2]. There is high confidence that increasing global warming can expand the
10 land area affected by increasing drought frequency and severity [3]. Furthermore, drought increases tree
11 mortality and triggers changes in land cover and, consequently, land use, thus impacting ecosystems [4].
12 Nevertheless, there is a lack of understanding of how the alteration in water supply and demand is affecting
13 land cover transformations.

14 Precipitation is the primary driver of drought and is intensified by temperature [5]. Drought impacts soil
15 moisture, hydrological regimes, and vegetation productivity. Initially, drought was commonly classified as
16 meteorological, hydrological, and agricultural [6]. Lately, [7] and [8] have given an updated definition of
17 drought for the Anthropocene, suggesting that it should be considered the feedback of humans' decisions
18 and activities that drives the anthropogenic drought. Even though it has been argued that those definitions
19 do not fully address the ecological dimensions of drought. [4] proposed the ecological drought definition as
20 "*an episodic deficit in water availability that drives ecosystems beyond thresholds of vulnerability, impacts*
21 *ecosystem services, and triggers feedback in natural and/or human systems*". Moreover, many ecological
22 studies have misinterpreted how to characterize drought, for example, sometimes considering "dry" condi-
23 tions as "drought" [9]. On the other hand, the AR6 [1] states that even if global warming is stabilized at
24 1.5°–2°C, many parts of the world will be impacted by more severe agricultural and ecological droughts.
25 Then, there is a challenge in conducting drought research, especially to evaluate its impact on ecosystems.

26 Chile has been facing a persistent rainfall deficit for more than a decade [10], which has impacted vegeta-
27 tion development [11] and the hydrological system [12]. Current drought conditions have affected crop
28 productivity [13, 14], forest development [15, 16], forest fire occurrence [17], land cover change [18], water
29 supply in watersheds [19], and have had economic impacts [20]. In 2019–2020, the drought severity reached
30 an extreme condition in Central Chile (30–34°S) not seen for at least 40 years, and the evidence indicates
31 that the impact is transversal to the land cover classes of forest, grassland, and cropland [11]. The prolonged
32 lack of precipitation in Central Chile is producing changes in ecosystem dynamics that must be studied.

33 For the spatiotemporal assessment of drought impact (i.e., by water supply and demand) on land cover
34 changes, we need climatic reliable variables such as precipitation, temperature, soil moisture, land cover, and
35 vegetation status. For developing countries like Chile, the weather networks present several disadvantages,
36 such as gaps, a short history, and low-quality data. Reanalysis data, as the ERA5-Land (ERA5L) [21]
37 provides hourly climatic information (precipitation, temperature, and soil moisture) without gaps since
38 1950 with global extension. ERA5L has already been used for drought assessment using the Standardized
39 Precipitation-Evapotranspiration Index (SPEI) [22] and for flash drought [23] by analyzing soil moisture
40 and evapotranspiration. On the other hand, satellite remote sensing [24, 25] is the primary method to
41 evaluate how drought impacts vegetation dynamics. Vegetation drought indices (VDI) are commonly used
42 as proxies of productivity [26, 27], which can be derived from the MODIS (Moderate-Resolution Imaging
43 Spectroradiometer). Besides, land use and land cover (LULC) change can be driven by drought [28, 29]. To
44 analyze these changes, multiple LULC products exist [30], one of those that provides time series since 2001
45 is the MCD12Q1 [31] from MODIS. The variation in water supply and demand is finally reflected in the
46 total water storage (TWS). The TWS can be retrieved by the Gravity Recovery and Climate Experiment
47 (GRACE), which allows analyzing water availability changes at coarse resolution [32, 33]. We can use climatic
48 reanalysis (ERA5L) and vegetation data (MODIS) to derive drought indices of supply (i.e., precipitation)
49 and demand (i.e., temperature) and thus evaluate the impact of drought on LULC changes. Further, the
50 TWS can be assessed with regard to the changes in water supply and demand to gain insight into the impact
51 on water storage.

52 To evaluate meteorological drought (i.e., water supply), the World Meteorological Organization (WMO;
53 [34]) recommends the Standardized Precipitation Index (SPI; [35]), a multiscalar drought index that allows
54 to monitor precipitation deficits from short- to long-term. Following the same approach, [36] incorporates

55 into the SPI the effect of temperature through the use of potential evapotranspiration, thus proposing the
56 SPEI (Standardized Precipitation Evapotranspiration Index). Similarly, to evaluate solely the evaporative
57 demand driven by temperature, [37] and [38] came up with the Evaporative Demand Drought Index (EDDI).
58 For vegetation, in a similar manner as the SPI, SPEI and EDDI; [14] proposed the zcNDVI, a standardized
59 anomaly of the cumulative Normalized Difference Vegetation Index (NDVI), which could be accumulated
60 over the growing season or any period (e.g., months), resulting in a multiscalar drought index. For soil
61 moisture, several drought indices exist, such as the Soil Moisture Deficit Index (SDMI) a normalized index
62 [39] and the Soil Moisture Agricultural Drought Index (SMADI) [40] which is a normalized index using
63 vegetation, land surface temperature, and a vegetation condition index (VCI, [41]). From TWS, we can
64 estimate the standardized terrestrial water storage index (STI) [42], a standardized anomaly that follows
65 the methodology of the SPI, SPEI, EDDI, and zcNDVI. Thereby, we have drought indices for water supply,
66 demand, and storage, which can help to make a comprehensive assessment of drought.

67 In this research, we present the raster dataset DDS4Chl, which provides climate variables and drought
68 indices of water demand and supply and vegetation productivity for continental Chile since 1981 at a
69 monthly frequency. Those were gathered from the earth observation products ERA5L and MODIS. Then,
70 we used DDS4Chl to analyze the impact of drought on different types of land cover classes in continental
71 Chile. The specific objectives of the study are: i) to analyze the trend on multi-scalar drought indices
72 for water demand and supply, soil moisture, and vegetation productivity for 1981–2023/2001–2023; ii) to
73 evaluate LULC change for 2001–2021 and its relation to drought indices; iii) to analyze the relationship of
74 a proxy of vegetation productivity (zcNDVI) with drought indices of water demand and supply and soil
75 moisture; and iv) to assess if the observed changes in the drought indices are linked to TWS.

76 2. Study area (AGREGAR SUPERFICIE DE LANDCOVER EN CADA MACROZONA)

77 Continetal Chile has a diverse climate condition from north to south and east to west [43] (Figure 1), which
78 determines its great ecosystem diversity (Figure 2). The Andes Mountains are a main factor in latitudinal
79 variation [44]. To describe the climate and ecosystem of Chile, we use the Koppen-Geiger release by [45] and
80 the landcover type persistance of 80% of times for 2001–2022, from the IGBP classification scheme [31] (see
81 Section 3.4). “Norte Grande” and “Norte Chico” predominate in an arid desert climate with hot (Bwh) and
82 cold (Bwk) temperatures. At the south of “Norte Chico,” the climate changes to an arid steppe with cold
83 temperatures (Bsk). Mainly, the land is barren, with a minor surface of vegetation types such as shrubland
84 and grassland. In the zones “Centro” and the north half of “Sur,” the main climate is Mediterranean, with
85 warmer to hot summers (Csa and Csb). In “Centro,” there is a major proportion (~50%) of chilean matorral
86 (shrubland and savanna, [18]), followed by grassland (~16%), forest (8%), and croplands (5%). The south
87 part of “Centro” and the north part of “Austral” are dominated by an Oceanic climate (Cfb). Those zones
88 are high in forest and grassland. The southern part of the country has a tundra climate, and in Patagonia,
89 it is a cold semi-arid area with an extended surface of grassland.

90 3. Materials and Methods

91 3.1. Software and packages used

92 For the downloading, processing, and analysis of the spatio-temporal data, we used the open source software
93 for statistical computing and graphics, R [46]. For downloading ERA5L, we used the {ecmwfr} package [47].
94 For processing raster data, we used {terra} [48] and {stars} [49]. For managing vectorial data, we used
95 {sf} [50]. For the calculation of AED, we used {SPEI} [51].

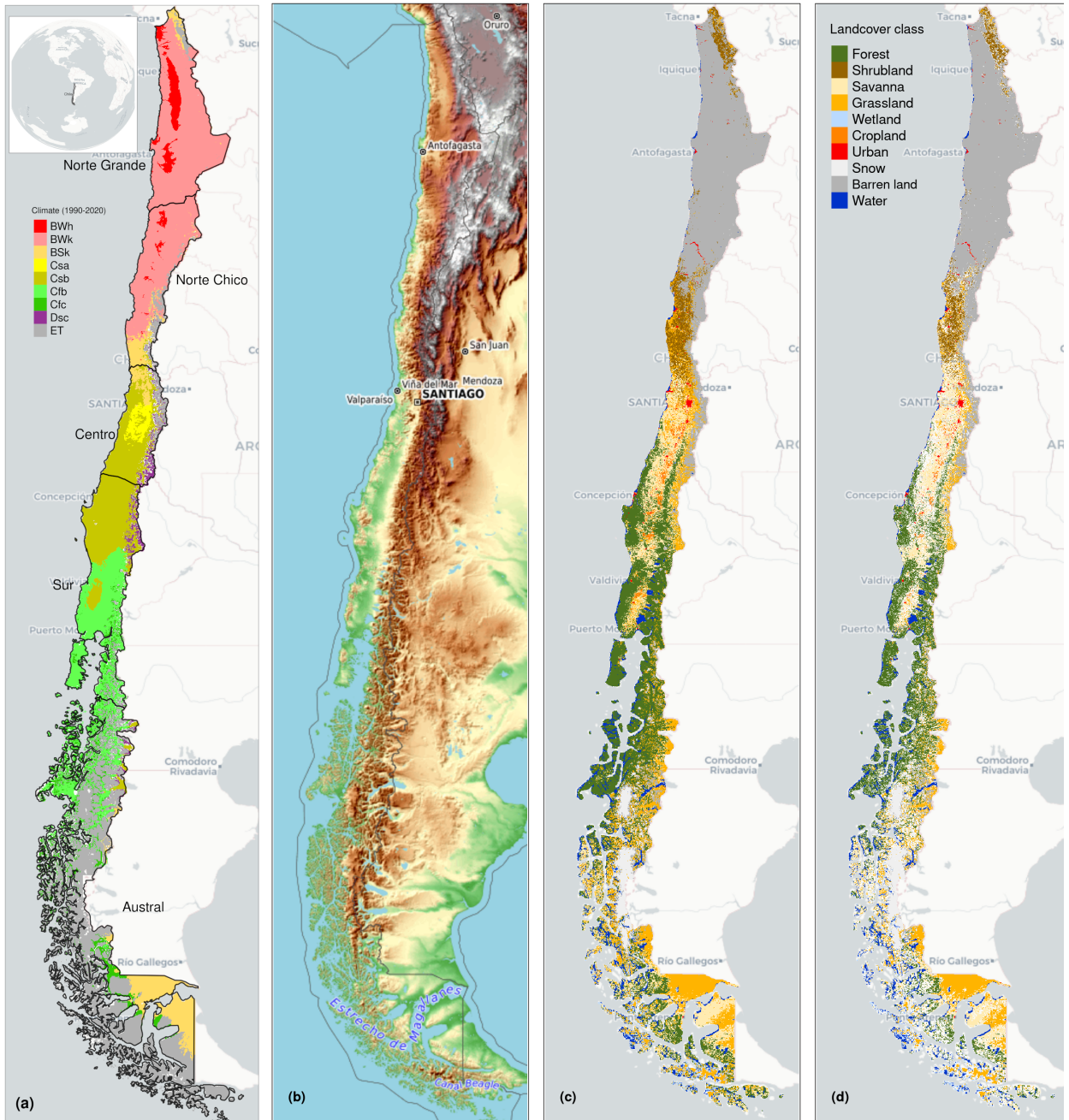


Figure 1: (a) Chile with the Koppen-Geiger climate classes and the five macrozones “Norte Grande”, “Norte Chico”, “Centro”, “Sur”, and “Austral”. (b) Topography reference map. (c) Land cover classes for 2022. (d) Persistent land cover classes (> 80%) for 2001-2022

96 3.2. Data

97 3.2.1. Earth observation data

98 For water supply and demand variables, we used ERA5L [21], a reanalysis dataset that provides the evolution
99 of land variables since 1950. It has a spatial resolution of 0.1° , hourly frequency, and global coverage. We

100 selected the variables for total precipitation, 2 meter temperature maximum and minimum, and volumetric
 101 soil water layers between 0 and 100cm of depth (layer 1 to layer 3). The data was downloaded using the
 102 Copernicus Climate Data Store (CDS) Application Program Interface (API) implemented in `{ecmwf}` [47].

103 To derive a proxy of vegetation productivity, we used the product MOD13A3 collection 6.1 from MODIS
 104 [52]. It provides vegetation indices (NDVI and EVI) at 1km of spatial resolution and monthly frequency. The
 105 MOD13A3.061 and MCD12Q1.061 were retrieved from the online Data Pool, courtesy of the NASA EOSDIS
 106 Land Processes Distributed Active Archive Center (LP DAAC), USGS Earth Resources Observation and
 107 Science (EROS) Center, Sioux Falls, South Dakota, <https://lpdaac.usgs.gov/tools/data-pool/>.

Table 1: Description of the earth observation data used

Product	Sub-product	Variable	Spatial Resolution	Period	Units	Short Name
ERA5L		Precipitation	0.1°	1981-2023	mm	P
		Maximum temperature			°C	T _{max}
		Minimum temperature			°C	T _{min}
		Volumetric Soil Water Content at 1m			m3/m3	SM
ERA5L*	MOD13A3.061	Atmospheric Evaporative Demand	0.1°	1981-2023	mm	AED
		Normalized Difference Vegetation Index			2000-2023	NDVI
MODIS	MCD12Q1.061	Landcover IGBP scheme	1 km	2001-2022		Landcover

*Derived from ERA5L with Eq. 1.

108 3.2.2. *in-situ* data

109 3.3. Drought Indices

110 We derived the drought indices of water supply and demand, soil moisture from the ERA5L dataset, and
 111 vegetation from the MODIS product, all at monthly frequency.

112 For the indices EDDI and SPEI that use water demand, first we have to calculate the AED. For this, we
 113 used the method of Hargreaves [53]:

$$AED = 0.0023 \cdot Ra \cdot (T + 17.8) \cdot (T_{max} - T_{min})^{0.5} \quad (1)$$

114 where Ra ($MJ m^2 day^{-1}$) is extraterrestrial radiation; T , T_{max} , and T_{min} are mean, maximum, and
 115 minimum temperature ($^{\circ}C$). We calculate the centroid coordinates per pixel and use the latitude to estimate
 116 Ra .

117 To evaluate water demand, we chose the EDDI [37, 38] index, which uses the AED. For supply, we used
 118 the index recommended by the World Meteorological Organization (WMO) for monitoring drought, the SPI
 119 [35]. We calculated the SPEI, which used a balance between P and AED , in this case, an auxiliary variable
 120 $D = P - AED$ is used. In this study, we used the SSI (standardized soil moisture index at 1 m) [54, 55],
 121 which uses SM. Finally, for the proxy of productivity, zcNDVI, we used the NDVI. Before using the NDVI,
 122 it was smoothed following the procedure described in [14] and [13].

123 All the indices are multi-scalar and were calculated for time scales of 1, 3, 6, 12, 24, and 36 months, except
 124 for zcNDVI, which was calculated for 6 months. The goal is to be able to evaluate short- and long-term
 125 droughts in water demand and supply and soil moisture. This is particularly important for central Chile
 126 because it has suffered from a prolonged decrease in precipitation for more than 12 years [56, 12, 10].

127 To calculate the drought indices, first we must calculate the accumulation of the variable. In this case, for
 128 generalization purposes, we will use V , referring to P , AED , D , $NDVI$, and SM (Table 1). We cumulated
 129 each V over the time series of n values, and for the time scales s :

$$A_{si} = \sum_{i=n-s-i+2}^{n-i+1} V_i \quad \forall i \geq n - s + 1 \quad (2)$$

130 It corresponds to a moving window (convolution) that sums the variable for s starting for the last month
 131 n until the month, which could sum for s months ($n-s+1$). Once the variable is cumulated over time for
 132 the scale s , we used a nonparametric approach following [37] to derive the drought indices. Thus, the
 133 empirically derived probabilities are obtained through an inverse normal approximation [57]. Then, we
 134 used the empirical Tukey plotting position [58] over A_i to derive the $P(A_i)$ probabilities across a period of
 135 interest:

$$P(A_i) = \frac{i - 0.33}{n + 0.33} \quad (3)$$

136 The drought indices *SPI*, *SPEI*, *EDDI*, *SSI*, and *zcNDVI* are obtained following the inverse normal
 137 approximation:

$$DI(A_i) = W - \frac{C_0 + C_1 \cdot W + c_2 \cdot W^2}{1 + d_1 \cdot W + d_2 \cdot W^2 + d_3 \cdot W^3} \quad (4)$$

138 DI is referring to the drought index calculated for the variable V . The values for the constats are:
 139 $C_0 = 2.515517$, $C_1 = 0.802853$, $C_2 = 0.010328$, $d_1 = 1.432788$, $d_2 = 0.189269$, and $d_3 = 0.001308$. For
 140 $P(A) \leq 0.5$, $W = \sqrt{-2 \cdot \ln(P(A_i))}$, and for $P(A_i) > 0.5$, replace $P(A_i)$ with $1 - P(A_i)$ and reverse the sign
 141 of $DI(A_i)$.

142 3.4. LULC change for 2001-2022 and its relation with water supply and demand, and soil moisture

143 To analyze the LULCC, we use the IGBP scheme from the MCD12Q1 collection 6.1 from MODIS. This
 144 product has a yearly frequency from 2001 to 2022. The IGBP defines 17 classes; from these, we regrouped
 145 into ten macroclasses for forest, schrublands, savannas, grasslands, wetlands, croplands, urban, snow and
 146 ice, barren, and water bodies. To validate the IGBP MODIS, we compare the macroclasses with the ones
 147 of a more detailed landcover map made by [59] for Chile for the years 2013–2014 (LCChile). The later has
 148 a spatial resolution of 30 m and three levels of defined classes; from those, we used level 1, which fits with
 149 the macroclasses derived from the IGBP MODIS. We chose the years 2013 and 2014 from MODIS IGBP
 150 because the LCChile was made with data acquired in 2013 and 2014. We resampled LCChile to the spatial
 151 resolution of the IGBP MODIS using the nearest neighbor method. Then, we took a random sample of
 152 1000 points within continental Chile and extracted the classes that fell within each point for LCCHILE,
 153 IGP2013, and IGP2014. Finally, we applied a confusion matrix and estimated the accuracy and F1 score as
 154 metrics of performance. The validation of IGP2013 and IGP2014 with LCChile reached similar metrics
 155 of performance, having an accuracy of 0.82 and a F1 score of 0.66 (see SS1).

156 Later, with the goal of analyzing vegetation areas less affected by landcover change, we calculated a raster
 157 mask for IGBP MODIS considering the classes that remain for more than 80% of the years (2001–2022),
 158 which allows us to identify the areas with no landcover change for the macroclasses. Figure 2 shows the
 159 summary of the proportion of surface per landcover class and macrozone, derived from the mask over
 160 continental Chile.

161 Further, we calculated the surface occupied per landcover class into the five macrozones (“Norte Grande”
 162 to “Austral”) per year. After that, we calculated the trend’s change in surface; we used the Sen’ slope [60]
 163 based on Mann-Kendall [61]. This way, we obtain a matrix of trends of 5 x 5 (macrozones x landcover).

164 We will explore if the trend in landcover classess is associated to trend of the drought indices. For this
 165 we will use the regularizations techniques of Lasso [62] and Ridge regression [63]. Also, we will test random
 166 forest for this purpose [64].

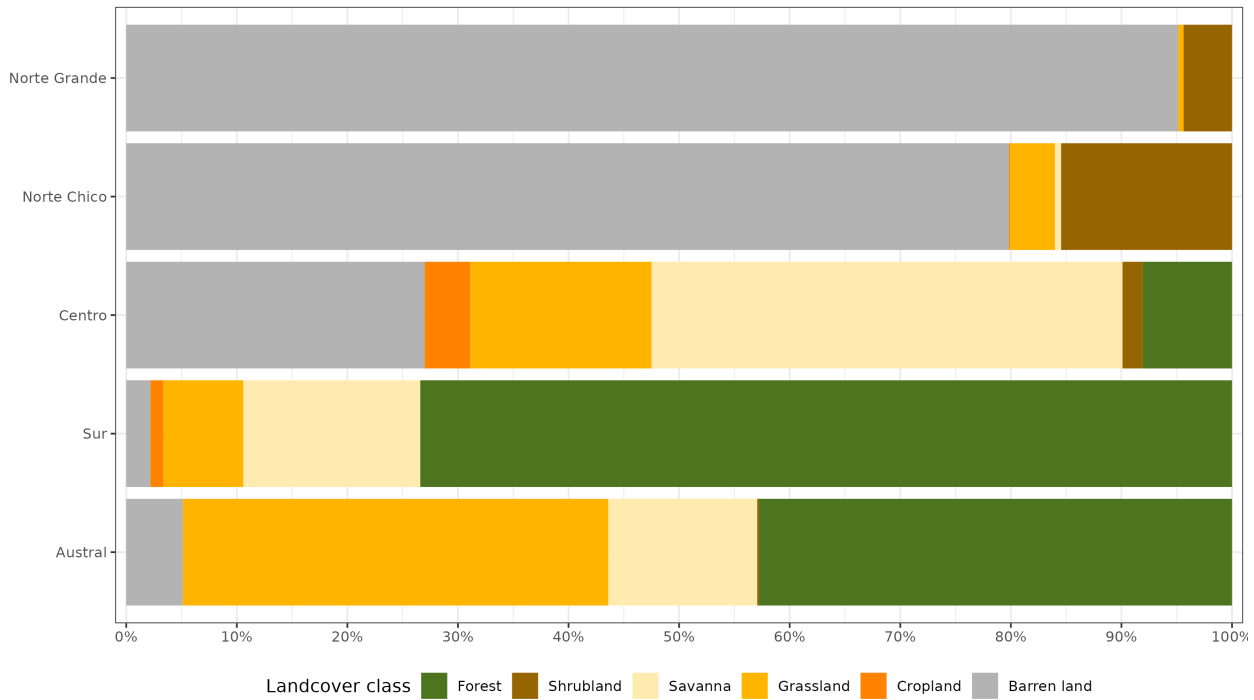


Figure 2: Proportion of land cover class from the persistent land cover for 2001-2022 (>80%) per macrozone

167 3.5. Trend of drought indices for water demand and supply, soil moisture, and vegetation productivity

168 To estimate if there are significant positive or negative trends for the drought indices, we used the non-
 169 parametric test of Mann-Kendall [61]. To determine the magnitude of the trend, we used Sen's slope [60].
 170 One of the advantages of applying this methodology is that the Sen's slope is not affected by outliers as
 171 regular regression does. We applied both to the six time scales from 1981 to 2023 (monthly frequency) and
 172 the indices SPI, EDDI, SPEI, and SSI. In the case of zcNDVI (six months) was for 2000 to 2023. Thus,
 173 we have 31 trends. Also, we extracted the trend aggregated by macrozone and landcover class, obtaining a
 174 table of 31x5x5 (drought indices trends x macrozone x landcover class). We will use this data in Section 3.4
 175 to analyze if there is a strong relationship between the trends of drought indices and land cover surface
 176 within continental Chile.

177 For zcNDVI, we want to remove the effect of the Andes's mountain and mask out trends that were at an
 178 elevation above 1500m because there is scarce vegetation.

179 [65] made a global analysis of the drought's severity trend using SPI, SPEI, and the Standardized Evap-
 180 otranspiration Deficit Index (SEDI; [66]) to evaluate AED. They indicate that the increase in hydrological
 181 drought has been due to anthropogenic effects rather than climate change. This is because the global in-
 182 crease in AED did not explain the change in the spatial pattern of the hydrological drought. Also, they state
 183 that "*the increase in hydrological droughts has been primarily observed in regions with high water demand*
 184 *and land cover change*". We will contrast this hypothesis with what is occurring in Chile. To achieve this,
 185 we will use the landcover class type that remains more than 80% of types for 2001–2022 to evaluate the
 186 trend on zcNDVI and use this as a mask where there are low changes.

187 3.6. Impact for water supply and demand, and soil moisture in vegetation productivity within landcover types

188 The aim of this section is to analyze the drought indices of water demand and supply and soil moisture
 189 against vegetation to address: i) if short- or long-term time scales are most important in impacting vegetation

through Chile; and ii) the strength of the correlation for the variable and the time scale. Then, we will summarize for each landcover class and macrozone. Thus, we will be able to advance in understanding how climate is affecting vegetation, considering the impact on the five macroclasses: forest, cropland, grassland, savanna, and shrubland.

To assess how water demand and supply and soil moisture are related to vegetation productivity (zcNDVI), we analyze the linear correlation between the indices SPI, SPEI, EDDI, and SSI for 1, 3, 6, 12, 24, and 36-month time scales against zcNDVI. We followed a similar approach to that used by [67] when using the SPI for meteorological drought against the cumulative FAPAR (Fraction of Absorbed Photosynthetically Active Radiation) as a proxy for vegetation productivity. We made a pixel-to-pixel linear correlation analysis per index. First, we calculate the Pearson coefficient of correlation for the six time scales and let the time scale that reaches the maximum correlation be significant ($p < 0.05$). Then, we extracted the Pearson correlation value corresponding to the time scales that reached the maximum value. Thus, we derived two raster maps per index, the first with the time scales and the second with the correlation value.

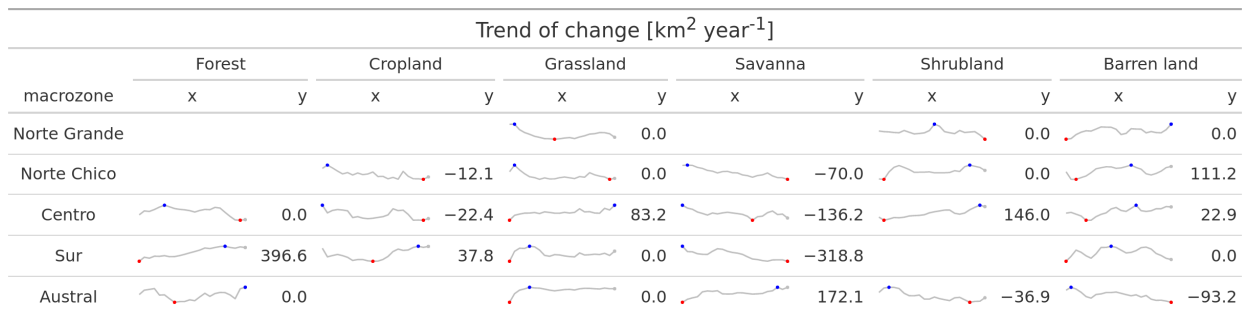
3.7. Validation of ERA5L variables

4. Results

4.1. LULC change for 2001-2022 and its relation with water supply and demand, and soil moisture

Figure 3 and ?? show that the macrozones with major LULCC for 2001-2022 were “Centro”, “Sur”, and “Austral” with 36%, 31%, and 34%, respectively. The “Norte Chico” shows an increase in barrend land of $111 \text{ km}^2 \text{year}^{-1}$ and a reduction in the class savanna $-70 \text{ km}^2 \text{year}^{-1}$. In the “Centro” and “Sur” there are changes in the chilean matorral, with an important reduction in savanna (-136 to $-318 \text{ km}^2 \text{yr}^{-1}$), and an increase in shrubland and grassland. Showing a change for more dense vegetation types. It appears to be a change from the surface occupied by cropland from the “Centro” to the “Sur.” Also, there is a high increase in forest ($397 \text{ km}^2 \text{yr}^{-1}$) in the “Sur,” replacing the savanna lost.

Table 2: The value of Sen’s slope trend next to the time-series plot of surface per landcover class (IGBP MCD12Q1.016) for 2001–2022 through Central Chile. Values of zero indicate that there was not a significant trend. Red dots on the plots indicate the maximum and minimum values of surface.



4.2. Trend of drought indices for water demand and supply, soil moisture, and vegetation productivity

Regarding vegetation productivity aggregated through the macrozones in the five landcover macroclasses. In “Norte Grande” there is a increase trend of 0.02 (z-index) per decade, related with types of grassland and shrubland. There is a negative trend in “Norte Chico” with -0.04 and “Centro” with -0.02 per decade. In the “Norte Chico,” savanna (-0.05) has the lowest trend, and the rest of the types are around -0.04. In “Centro,” shrubland reaches -0.06, followed by grassland with -0.05, and croplands and savanna have ~ 0.01 per decade. This could be associated either with a reduction in vegetation surface, a decrease in biomass,

220 or browning [68]. Vegetation reached its lowest values since the year 2019, reaching an extreme condition
 221 in early 2020 and 2022 in the “Norte Chico” and Centro” (Mega Drought). The “Sur” and “Austral” show
 222 a positive trend of around 0.016 per decade (Figure 3). The area most affected by a negative trend in
 223 vegetation seems to be associated with the Chilean matorral [18], despite the croplands being as severely
 224 impacted by drought as native vegetation does in “Norte Chico.”

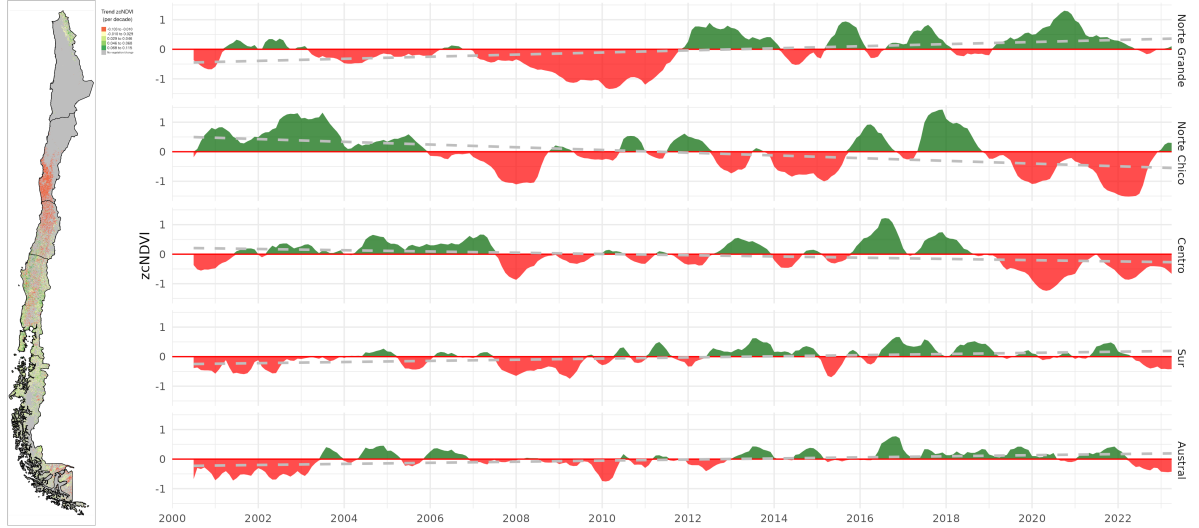


Figure 3: (a) Map of the linear trend of the index zcNDVI-6 for 2001–2023. Greener colors indicate a positive trend; redder colors correspond to a negative trend and a decrease in vegetation productivity. Grey colors indicate either no vegetation or a change in landcover type for 2001–2022. (b) Temporal variation of zcNDVI-6 aggregated at macrozone level within continental Chile. Each horizontal panel corresponds to a macrozone from ‘Norte Grande’ to ‘Austral’.

225 Analyzing the water supply in the macrozones “norte chico,” “central,” and “sur,” the SPI shows a de-
 226 creasing trend that increases at longer time scales due to the prolonged reduction in precipitation. It reaches
 227 a trend of -0.056 (z-score) per decade (Figure 4) for time scales of 36 months. In the case of water demand,
 228 we analyze the EDDI. It shows a positive trend, caused by an increase in AED. The trend on EDDI reaches
 229 a maximum of 0.053 per decade in the macrozones “norte grande” and “norte chico” (**?@fig-trendEDDI**).
 230 The behavior is similar to SPI, having close trends with opposite signs. Nevertheless, the spatial patterns
 231 are different. The maximum trend for SPI-36 is in “norte chico” and “zona central.” For EDDI-36, the
 232 maximum trend is from “northe grande” to “zona central.”

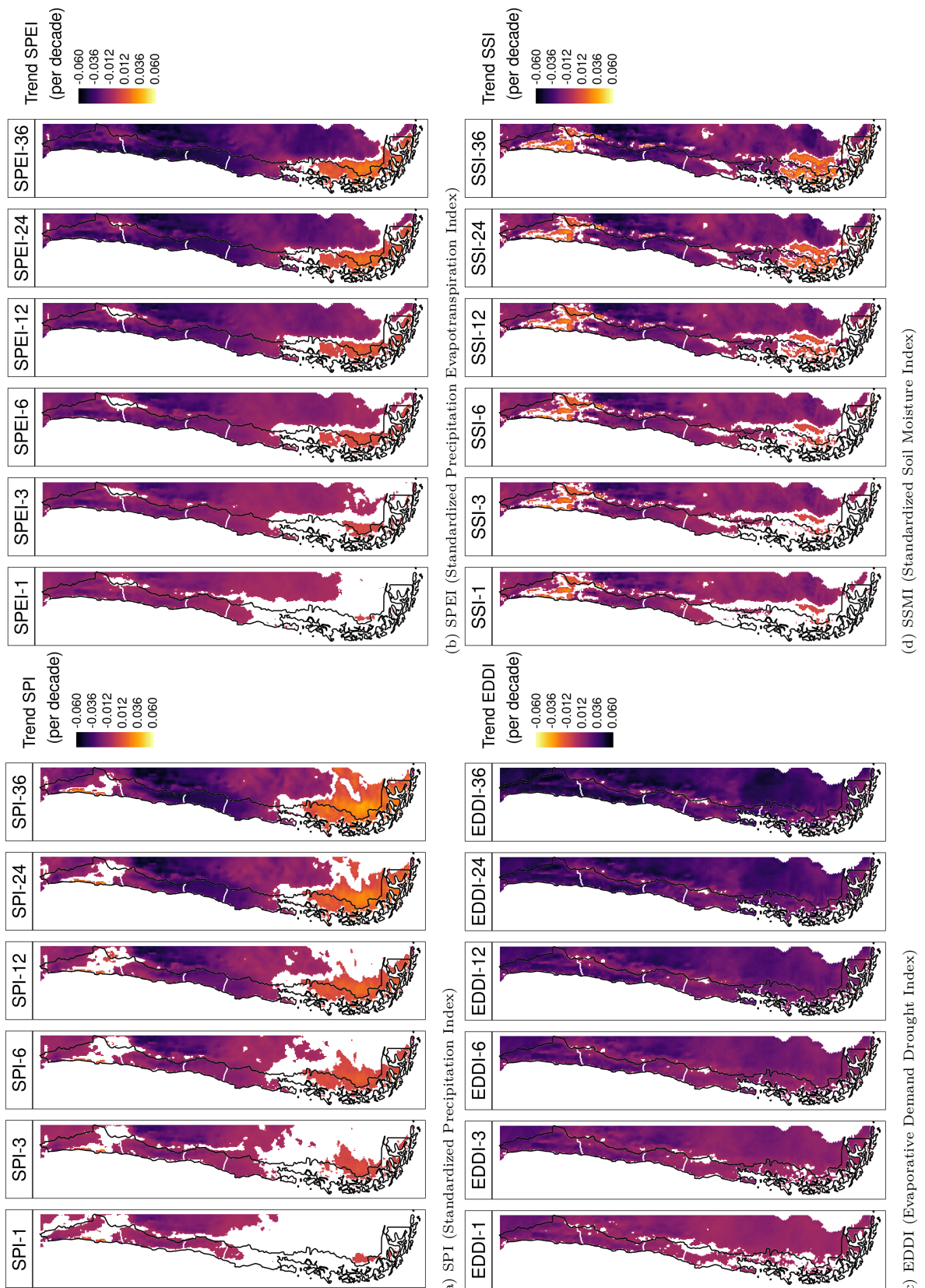
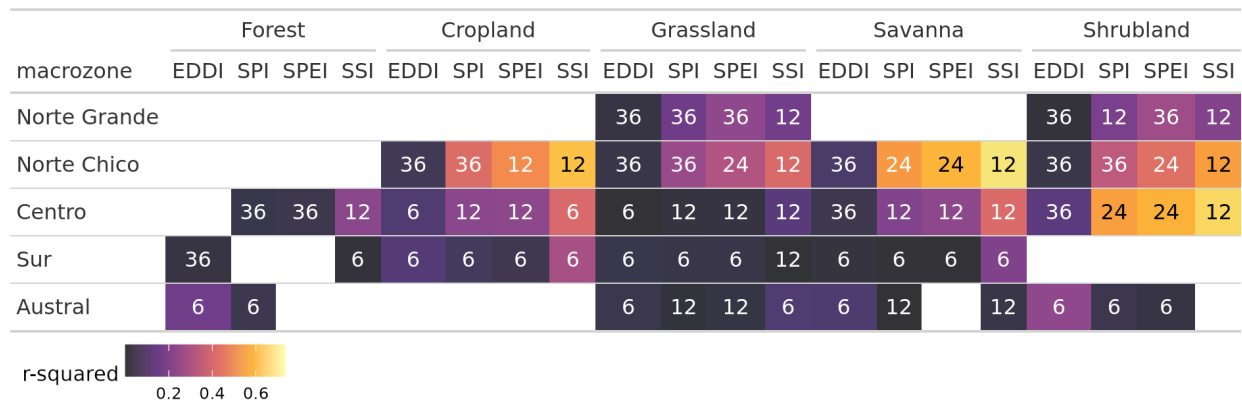


Figure 4: Linear trend of the drought index (*) at time scales of 1, 3, 6, 12, 24, and 36 months for 1981-2023

233 4.3. Impact for water supply and demand, and soil moisture in vegetation productivity (CHEQUEAR
 234 CIFRAS EN EL TEXTO)

235 According with what is showed Figure 5, Figure 6, and Table 3. Forest seems to be the most resistant
 236 type to drought, showing that only “Centro” is slightly ($rsq = 0.3$) impacted by a 12-month soil moisture
 237 deficit (SSI-12). Following by grasslands, which show to be impacted by a SSI-12 with a $rsq = 0.4$, and a
 238 decrease in water supply (SPI-36 and SPEI-24 with $rsq = 0.3$) in the “Norte Chico” and to a lesser degree
 239 in the “Norte Grande.” But, in the southern macrozones, this type was not affected by water demand,
 240 water supply, or soil moisture. The types that show to be most affected by variation in climate conditions
 241 are shrublands, savannas, and croplands. For savanna in “Norte Chico,” the SSI-12 and SPI-24 reached
 242 an rsq of 0.8 and 0.6, respectively. This value decreases to the south, but the SSI-12 is still the variable
 243 explaining more of the variation in vegetation productivity ($rsq = 0.4$ in “Centro” and 0.2 in “Sur”). In the
 244 case of croplands, the SPEI-12, SPI-36, and SSI-12 explain between 40% and 75% in “Centro.” The most
 245 affected type by climatic variation was shrubland, where in “Norte Chico” and “Centro” soil moisture and
 246 precipitation explained more than 50%, with SSI-12 being the most relevant variable, followed by SPI-36 in
 247 “Norte Chico” and SPI-24 in “Sur.”

Table 3: Summary per landcover macroclass and macrozone regarding the correlation between zcNDVI with the drought indices EDDI, SPI, SPEI, and SSI for time scales of 1, 3, 6, 12, 24, and 36. The numbers in each cell indicate the time scale that reached the maximum correlation for the landcover and macrozone, and the color indicates the strength of the r-squared obtained with the index and the time scale.



248 4.4. Validation of ERA5L variables

249 5. Discussion

250 1.- Respecto a lo que indica [66], de que el aumento en la tendencia en severidad de la sequía (hidrológica)
 251 tiene que ver más con un aumento de la demanda de agua (LULCC) que a una tendencia en las condiciones
 252 climáticas (SPI-12).

253 2.- Sobre los tipos de landcover más afectados por los indicadores de sequía. Asociación con el matorral
 254 chileno [18]. Diferencia entre el Norte Chico y Centro y lo que pasa hacia el sur.

255 3. Como podrían servir estos resultados para desarrollar un predictor de sequía basado.

256 4.- Qué se podría hacer mejor en futuras investigaciones del tema.

257 5.- Sequía, aridez, water scarcity. Si puede utilizar el mapa y proyección climática de Koppen_Geiger [45]
 258 para dirigir esta discusión

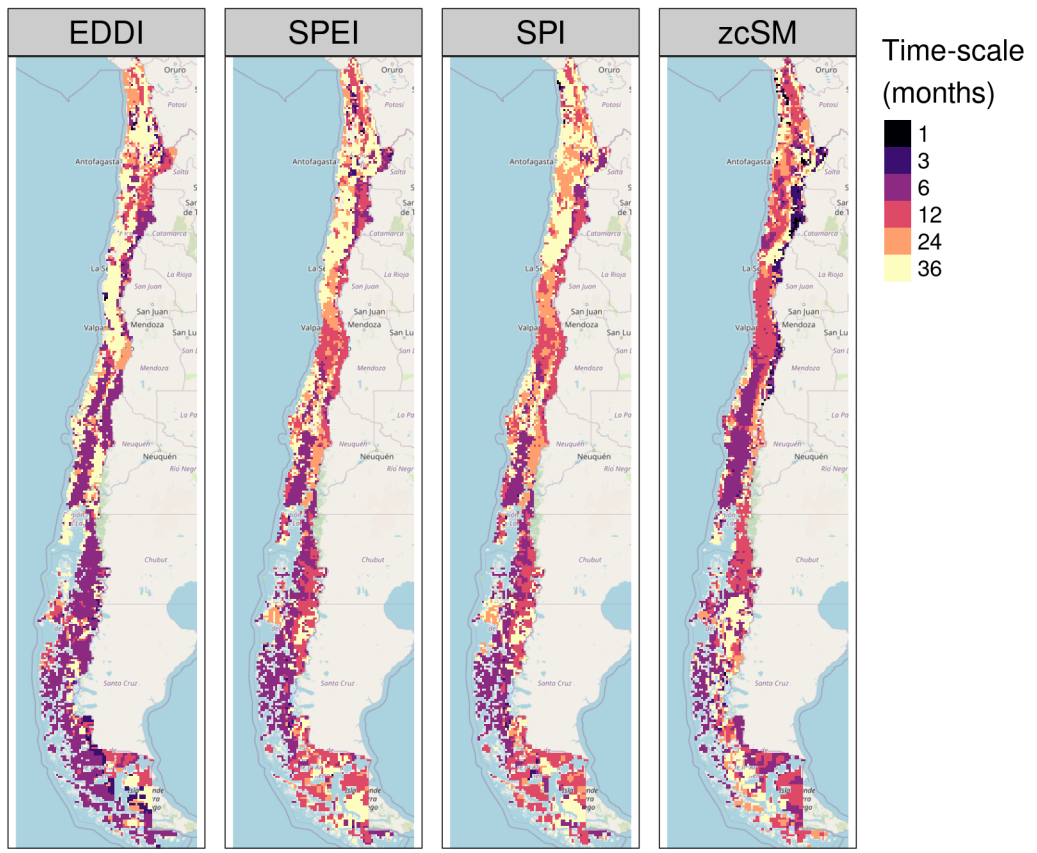


Figure 5: Time scales per drought index that reach the maximum coefficient of determination

259 **6. Conclusion**

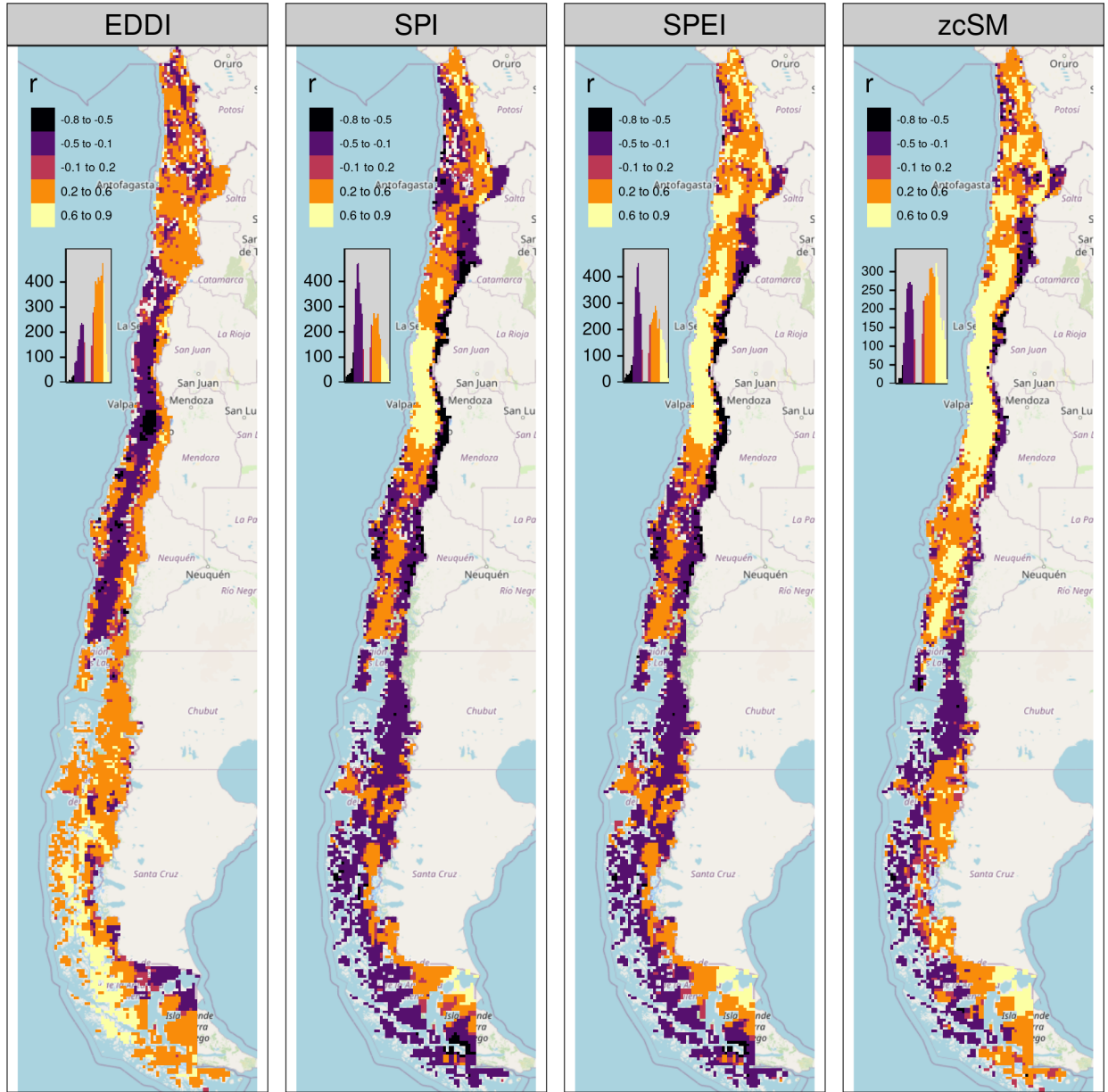


Figure 6: Pearson correlation value for the time scales and drought index that reach the maximum coefficient of determination

260 References

- 261 [1] K. Calvin, D. Dasgupta, G. Krinner, A. Mukherji, P. W. Thorne, C. Trisos, J. Romero, P. Aldunce, K. Barrett, G. Blanco,
 262 W. W. Cheung, S. Connors, F. Denton, A. Diongue-Niang, D. Dodman, M. Garschagen, O. Geden, B. Hayward, C. Jones,
 263 F. Jotzo, T. Krug, R. Lasco, Y.-Y. Lee, V. Masson-Delmotte, M. Meinshausen, K. Mintenbeck, A. Mokssit, F. E. Otto,
 264 M. Pathak, A. Pirani, E. Poloczanska, H.-O. Pörtner, A. Revi, D. C. Roberts, J. Roy, A. C. Ruane, J. Skea, P. R.
 265 Shukla, R. Slade, A. Slangen, Y. Sokona, A. A. Sörensson, M. Tignor, D. Van Vuuren, Y.-M. Wei, H. Winkler, P. Zhai,
 266 Z. Zommers, J.-C. Hourcade, F. X. Johnson, S. Pachauri, N. P. Simpson, C. Singh, A. Thomas, E. Totin, P. Arias,
 267 M. Bustamante, I. Elgizouli, G. Flato, M. Howden, C. Méndez-Vallejo, J. J. Pereira, R. Pichs-Madruga, S. K. Rose,
 268 Y. Saheb, R. Sánchez Rodríguez, D. Ürge Vorsatz, C. Xiao, N. Yassaa, A. Alegria, K. Armour, B. Bednar-Friedl, K. Blok,
 269 G. Cissé, F. Dentener, S. Eriksen, E. Fischer, G. Garner, C. Guiuarch, M. Haasnoot, G. Hansen, M. Hauser, E. Hawkins,
 270 T. Hermans, R. Kopp, N. Leprince-Ringuet, J. Lewis, D. Ley, C. Ludden, L. Niamir, Z. Nicholls, S. Some, S. Szopa,

- 271 B. Trewin, K.-I. Van Der Wijst, G. Winter, M. Witting, A. Birt, M. Ha, J. Romero, J. Kim, E. F. Haites, Y. Jung,
 272 R. Stavins, A. Birt, M. Ha, D. J. A. Orendain, L. Ignon, S. Park, Y. Park, A. Reisinger, D. Cammarano, A. Fischlin, J. S.
 273 Fuglestvedt, G. Hansen, C. Ludden, V. Masson-Delmotte, J. R. Matthews, K. Mintenbeck, A. Pirani, E. Poloczanska,
 274 N. Leprince-Ringuet, C. Péan, IPCC, 2023: Climate Change 2023: Synthesis Report. Contribution of Working Groups I,
 275 II and III to the Sixth Assessment Report of the Intergovernmental Panel on Climate Change [Core Writing Team, H.
 276 Lee and J. Romero (eds.)]. IPCC, Geneva, Switzerland., Tech. rep., Intergovernmental Panel on Climate Change (IPCC)
 277 (Jul. 2023).
 278 URL <https://www.ipcc.ch/report/ar6/syr/>
- 279 [2] IPCC, Climate Change 2013: The Physical Science Basis. Contribution of Working Group I to the Fifth Assessment Report
 280 of the Intergovernmental Panel on Climate Change, Cambridge University Press, Cambridge, UK; New York, USA, 2013.
 281 doi:[10.1017/CBO9781107415324](https://doi.org/10.1017/CBO9781107415324).
 282 URL www.climatechange2013.org
- 283 [3] X. a. A. M. a. B. W. a. D. C. a. L. a. A. G. S. a. I. I. a. K. J. a. L. S. a. O. F. a. P. I. a. S. M. a. V.-S. S. a. W. M. a. Z. .
 284 M.-D. B. a. V. a. O. Seneviratne, S and Zhang, Weather and Climate Extreme Events in a Changing Climate, Cambridge
 285 University Press. In Press., 2021, publication Title: Climate Change 2021: The Physical Science Basis. Contribution of
 286 Working Group I to the Sixth Assessment Report of the Intergovernmental Panel on Climate Change.
- 287 [4] S. D. Crasbaw, A. R. Ramirez, S. L. Carter, M. S. Cross, K. R. Hall, D. J. Bathke, J. L. Betancourt, S. Colt, A. E. Cravens,
 288 M. S. Dalton, J. B. Dunham, L. E. Hay, M. J. Hayes, J. McEvoy, C. A. McNutt, M. A. Moritz, K. H. Nislow, N. Raheem,
 289 T. Sanford, Defining Ecological Drought for the Twenty-First Century, Bulletin of the American Meteorological Society
 290 98 (12) (2017) 2543–2550, publisher: American Meteorological Society. doi:[10.1175/BAMS-D-16-0292.1](https://doi.org/10.1175/BAMS-D-16-0292.1).
 291 URL <https://journals.ametsoc.org/view/journals/bams/98/12/bams-d-16-0292.1.xml>
- 292 [5] L. Luo, D. Apps, S. Arcand, H. Xu, M. Pan, M. Hoerling, Contribution of temperature and precipitation anomalies to the
 293 California drought during 2012–2015, Geophysical Research Letters 44 (7) (2017) 3184–3192. doi:[10.1002/2016GL072027](https://doi.org/10.1002/2016GL072027).
 294 URL <https://agupubs.onlinelibrary.wiley.com/doi/10.1002/2016GL072027>
- 295 [6] D. A. Wilhite, M. H. Glantz, Understanding: The drought phenomenon: The role of definitions, Water International
 296 10 (3) (1985) 111–120. doi:[10.1080/02508068508686328](https://doi.org/10.1080/02508068508686328).
 297 URL <http://dx.doi.org/10.1080/02508068508686328>
- 298 [7] A. F. Van Loon, T. Gleeson, J. Clark, A. I. Van Dijk, K. Stahl, J. Hannaford, G. Di Baldassarre, A. J. Teuling, L. M.
 299 Tallaksen, R. Uijlenhoet, D. M. Hannah, J. Sheffield, M. Svoboda, B. Verbeiren, T. Wagener, S. Rangecroft, N. Wanders,
 300 H. A. Van Lanen, Drought in the Anthropocene, Nature Geoscience 9 (2) (2016) 89–91. doi:[10.1038/ngeo2646](https://doi.org/10.1038/ngeo2646).
- 301 [8] A. AghaKouchak, A. Mirchi, K. Madani, G. Di Baldassarre, A. Nazemi, A. Alborzi, H. Anjileli, M. Azarderakhsh,
 302 F. Chiang, E. Hassanzadeh, L. S. Huning, I. Mallakpour, A. Martinez, O. Mazdiyasni, H. Moftakhari, H. Norouzi,
 303 M. Sadegh, D. Sadeqi, A. F. Van Loon, N. Wanders, Anthropogenic Drought: Definition, Challenges, and Opportunities,
 304 Reviews of Geophysics 59 (2) (2021) e2019RG000683. doi:[10.1029/2019RG000683](https://doi.org/10.1029/2019RG000683).
 305 URL <https://agupubs.onlinelibrary.wiley.com/doi/10.1029/2019RG000683>
- 306 [9] I. J. Slette, A. K. Post, M. Awad, T. Even, A. Punzalan, S. Williams, M. D. Smith, A. K. Knapp, How ecologists define
 307 drought, and why we should do better, Global Change Biology 25 (10) (2019) 3193–3200. doi:[10.1111/gcb.14747](https://doi.org/10.1111/gcb.14747).
 308 URL <https://onlinelibrary.wiley.com/doi/10.1111/gcb.14747>
- 309 [10] R. Garreaud, C. Alvarez-Garreton, J. Barichivich, J. P. Boisier, D. Christie, M. Galleguillos, C. LeQuesne, J. McPhee,
 310 M. Zambrano-Bigiarini, The 2010–2015 mega drought in Central Chile: Impacts on regional hydroclimate and vegetation,
 311 Hydrology and Earth System Sciences Discussions 2017 (2017) 1–37. doi:[10.5194/hess-2017-191](https://doi.org/10.5194/hess-2017-191).
 312 URL <http://www.hydrol-earth-syst-sci-discuss.net/hess-2017-191/>
- 313 [11] F. Zambrano, Four decades of satellite data for agricultural drought monitoring throughout the growing season in Central
 314 Chile, in: R. M. Vijay P. Singh Deepak Jhajharia, R. Kumar (Eds.), Integrated Drought Management, Two Volume Set,
 315 CRC Press, 2023, p. 28.
- 316 [12] J. P. Boisier, C. Alvarez-Garreton, R. R. Cordero, A. Damiani, L. Gallardo, R. D. Garreaud, F. Lambert, C. Ramallo,
 317 M. Rojas, R. Rondanelli, Anthropogenic drying in central-southern Chile evidenced by long-term observations and climate
 318 model simulations, Elementa 6 (1) (2018) 74. doi:[10.1525/elementa.328](https://doi.org/10.1525/elementa.328).
 319 URL <https://www.elementascience.org/article/10.1525/elementa.328/>
- 320 [13] F. Zambrano, M. Lillo-Saavedra, K. Verbist, O. Lagos, Sixteen years of agricultural drought assessment of the biobío
 321 region in chile using a 250 m resolution vegetation condition index (VCI), Remote Sensing 8 (6) (2016) 1–20, publisher:
 322 Multidisciplinary Digital Publishing Institute. doi:[10.3390/rs8060530](https://doi.org/10.3390/rs8060530).
 323 URL <http://www.mdpi.com/2072-4292/8/6/530>
- 324 [14] F. Zambrano, A. Vrieling, A. Nelson, M. Meroni, T. Tadesse, Prediction of drought-induced reduction of agricultural
 325 productivity in Chile from MODIS, rainfall estimates, and climate oscillation indices, Remote Sensing of Environment 219
 326 (2018) 15–30, publisher: Elsevier. doi:[10.1016/j.rse.2018.10.006](https://doi.org/10.1016/j.rse.2018.10.006).
 327 URL <https://www.sciencedirect.com/science/article/pii/S0034425718304541>
- 328 [15] A. Miranda, A. Lara, A. Altamirano, C. Di Bella, M. E. González, J. Julio Camarero, Forest browning trends in response
 329 to drought in a highly threatened mediterranean landscape of South America, Ecological Indicators 115 (2020) 106401.
 330 doi:[10.1016/j.ecolind.2020.106401](https://doi.org/10.1016/j.ecolind.2020.106401).
 331 URL <https://linkinghub.elsevier.com/retrieve/pii/S1470160X20303381>
- 332 [16] A. Venegas-González, F. R. Juñent, A. G. Gutiérrez, M. T. Filho, Recent radial growth decline in response to increased
 333 drought conditions in the northernmost Nothofagus populations from South America, Forest Ecology and Management
 334 409 (2018) 94–104. doi:[10.1016/j.foreco.2017.11.006](https://doi.org/10.1016/j.foreco.2017.11.006).
 335 URL <https://linkinghub.elsevier.com/retrieve/pii/S0378112717313993>

- 336 [17] R. Urrutia-Jalabert, M. E. González, . González-Reyes, A. Lara, R. Garreaud, [Climate variability and forest fires in](#)
 337 [central and south-central Chile](#), *Ecosphere* 9 (4) (2018) e02171. [doi:10.1002/ecs2.2171](#).
 338 URL <https://esajournals.onlinelibrary.wiley.com/doi/10.1002/ecs2.2171>
- 339 [18] I. Fuentes, R. Fuster, D. Avilés, W. Vervoort, [Water scarcity in central Chile: the effect of climate and land cover changes](#)
 340 [on hydrologic resources](#), *Hydrological Sciences Journal* 66 (6) (2021) 1028–1044. [doi:10.1080/02626667.2021.1903475](#).
 341 URL <https://www.tandfonline.com/doi/full/10.1080/02626667.2021.1903475>
- 342 [19] C. Alvarez-Garretón, J. P. Boisier, R. Garreaud, J. Seibert, M. Vis, [Progressive water deficits during multiyear droughts](#)
 343 [in basins with long hydrological memory in Chile](#), *Hydrology and Earth System Sciences* 25 (1) (2021) 429–446. [doi:](#)
 344 [10.5194/hess-25-429-2021](#).
 345 URL <https://hess.copernicus.org/articles/25/429/2021/>
- 346 [20] F. J. Fernández, F. Vásquez-Lavín, R. D. Ponce, R. Garreaud, F. Hernández, O. Link, F. Zambrano, M. Hanemann, [The](#)
 347 [economics impacts of long-run droughts: Challenges, gaps, and way forward](#), *Journal of Environmental Management* 344
 348 (2023) 118726. [doi:10.1016/j.jenvman.2023.118726](#).
 349 URL <https://linkinghub.elsevier.com/retrieve/pii/S0301479723015141>
- 350 [21] J. Muñoz-Sabater, E. Dutra, A. Agustí-Panareda, C. Albergel, G. Arduini, G. Balsamo, S. Bousetta, M. Choulga,
 351 S. Harrigan, H. Hersbach, B. Martens, D. G. Miralles, M. Piles, N. J. Rodríguez-Fernández, E. Zsotér, C. Buontempo,
 352 J.-N. Thépaut, [ERA5-Land: a state-of-the-art global reanalysis dataset for land applications](#), *Earth System Science Data*
 353 13 (9) (2021) 4349–4383. [doi:10.5194/essd-13-4349-2021](#).
 354 URL <https://essd.copernicus.org/articles/13/4349/2021/>
- 355 [22] M. Nouri, [Drought Assessment Using Gridded Data Sources in Data-Poor Areas with Different Aridity Conditions](#), *Water*
 356 *Resources Management* 37 (11) (2023) 4327–4343. [doi:10.1007/s11269-023-03555-4](#).
 357 URL <https://link.springer.com/10.1007/s11269-023-03555-4>
- 358 [23] M. Wang, L. Menzel, S. Jiang, L. Ren, C.-Y. Xu, H. Cui, [Evaluation of flash drought under the impact of heat wave events](#)
 359 [in southwestern Germany](#), *Science of The Total Environment* 904 (2023) 166815. [doi:10.1016/j.scitotenv.2023.166815](#).
 360 URL <https://linkinghub.elsevier.com/retrieve/pii/S0048969723054402>
- 361 [24] H. West, N. Quinn, M. Horswell, [Remote sensing for drought monitoring \& impact assessment: Progress, past challenges](#)
 362 [and future opportunities](#), *Remote Sensing of Environment* 232, publisher: Elsevier Inc. (Oct. 2019). [doi:10.1016/j.rse.2019.111291](#).
- 363 [25] A. AghaKouchak, A. Farahmand, F. S. Melton, J. Teixeira, M. C. Anderson, B. D. Wardlow, C. R. Hain, [Remote](#)
 364 [sensing of drought: Progress, challenges and opportunities](#), *Reviews of Geophysics* 53 (2) (2015) 452–480. [doi:10.1002/2014RG000456](#).
 365 URL <http://dx.doi.org/10.1002/2014RG000456>.
- 366 [26] J. M. Paruelo, M. Texeira, L. Staiano, M. Mastrángelo, L. Amdan, F. Gallego, [An integrative index of Ecosystem Services](#)
 367 [provision based on remotely sensed data](#), *Ecological Indicators* 71 (2016) 145–154, publisher: Elsevier. [doi:10.1016/J.ECOLIND.2016.06.054](#).
 368 URL <https://www.sciencedirect.com/science/article/pii/S1470160X16303843>
- 369 [27] A. Schucknecht, M. Meroni, F. Kayitakire, A. Boureima, A. Schucknecht, M. Meroni, F. Kayitakire, A. Boureima,
 370 [Phenology-Based Biomass Estimation to Support Rangeland Management in Semi-Arid Environments](#), *Remote Sensing* 9 (5) (2017) 463, publisher: Multidisciplinary Digital Publishing Institute. [doi:10.3390/rs9050463](#).
 371 URL <http://www.mdpi.com/2072-4292/9/5/463>
- 372 [28] H. T. Tran, J. B. Campbell, R. H. Wynne, Y. Shao, S. V. Phan, [Drought and Human Impacts on Land Use and Land](#)
 373 [Cover Change in a Vietnamese Coastal Area](#), *Remote Sensing* 2019, Vol. 11, Page 333 11 (3) (2019) 333, publisher:
 374 Multidisciplinary Digital Publishing Institute. [doi:10.3390/RS11030333](#).
 375 URL <https://www.mdpi.com/2072-4292/11/3/333.htm>
- 376 [29] F. O. Akinyemi, [Vegetation Trends, Drought Severity and Land Use-Land Cover Change during the Growing Season](#)
 377 [in Semi-Arid Contexts](#), *Remote Sensing* 2021, Vol. 13, Page 836 13 (5) (2021) 836, publisher: Multidisciplinary Digital
 378 Publishing Institute. [doi:10.3390/RS13050836](#).
 379 URL <https://www.mdpi.com/2072-4292/13/5/836.htm>
- 380 [30] G. Grekousis, G. Mountakis, M. Kavouras, [An overview of 21 global and 43 regional land-cover mapping products](#),
 381 *International Journal of Remote Sensing* 36 (21) (2015) 5309–5335. [doi:10.1080/01431161.2015.1093195](#).
 382 URL <https://www.tandfonline.com/doi/full/10.1080/01431161.2015.1093195>
- 383 [31] M. Friedl, D. Sulla-Menashe, MCD12Q1 MODIS/Terra+Aqua Land Cover Type Yearly L3 Global 500m SIN Grid V006
 384 [Data set]. NASA EOSDIS Land Processes DAAC (2019). [doi:10.5067/MODIS/MCD12Q1.006](#).
- 385 [32] M. Ahmed, M. Sultan, J. Wahl, E. Yan, [The use of GRACE data to monitor natural and anthropogenic induced variations](#)
 386 [in water availability across Africa](#), *Earth-Science Reviews* 136 (2014) 289–300, publisher: Elsevier. [doi:10.1016/J.EARSCIREV.2014.05.009](#).
- 387 [33] S. Ma, Q. Wu, J. Wang, S. Zhang, [Temporal Evolution of Regional Drought Detected from GRACE TWSA and CCI](#)
 388 [SM in Yunnan Province, China](#), *Remote Sensing* 2017, Vol. 9, Page 1124 9 (11) (2017) 1124, publisher: Multidisciplinary
 389 Publishing Institute. [doi:10.3390/RS9111124](#).
 390 URL <https://www.mdpi.com/2072-4292/9/11/1124.htm>
- 391 [34] WMO, M. Svoboda, M. Hayes, D. A. Wood, [Standardized Precipitation Index User Guide](#), WMO, Geneva, 2012, series
 392 Title: WMO Publication Title: WMO-No. 1090 © Issue: 1090.
 393 URL http://library.wmo.int/opac/index.php?lvl=notice_display&id=13682
- 394 [35] T. B. McKee, N. J. Doesken, J. Kleist, [The relationship of drought frequency and duration to time scales](#). In: *Proceedings*
 395 [of the Ninth Conference on Applied Climatology](#), American Meteorological Society (Boston) (1993) 179–184.

- 401 [36] S. M. Vicente-Serrano, S. Beguería, J. I. López-Moreno, **A multiscalar drought index sensitive to global warming: The stan-**
 402 **dardized precipitation evapotranspiration index**, Journal of Climate 23 (7) (2010) 1696–1718. [doi:10.1175/2009JCLI2909.1](https://doi.org/10.1175/2009JCLI2909.1).
 403
 404 URL <http://dx.doi.org/10.1175/2009JCLI2909.1>
- 405 [37] M. T. Hobbins, A. Wood, D. J. McEvoy, J. L. Huntington, C. Morton, M. Anderson, C. Hain, **The Evaporative Demand**
 406 **Drought Index. Part I: Linking Drought Evolution to Variations in Evaporative Demand**, Journal of Hydrometeorology
 407 17 (6) (2016) 1745–1761. [doi:10.1175/JHM-D-15-0121.1](https://doi.org/10.1175/JHM-D-15-0121.1).
 408 URL <http://journals.ametsoc.org/doi/10.1175/JHM-D-15-0121.1>
- 409 [38] D. J. McEvoy, J. L. Huntington, M. T. Hobbins, A. Wood, C. Morton, M. Anderson, C. Hain, **The Evaporative Demand**
 410 **Drought Index. Part II: CONUS-Wide Assessment against Common Drought Indicators**, Journal of Hydrometeorology
 411 17 (6) (2016) 1763–1779. [doi:10.1175/JHM-D-15-0122.1](https://doi.org/10.1175/JHM-D-15-0122.1).
 412 URL <http://journals.ametsoc.org/doi/10.1175/JHM-D-15-0122.1>
- 413 [39] B. Narasimhan, R. Srinivasan, Development and evaluation of Soil Moisture Deficit Index (SMDI) and Evapotranspiration
 414 Deficit Index (ETDI) for agricultural drought monitoring, Agricultural and Forest Meteorology 133 (1-4) (2005) 69–88.
 415 [doi:10.1016/j.agrformet.2005.07.012](https://doi.org/10.1016/j.agrformet.2005.07.012).
 416 URL <https://linkinghub.elsevier.com/retrieve/pii/S0168192305001565>
- 417 [40] A. G. S. S. Souza, A. Ribeiro Neto, L. L. D. Souza, **Soil moisture-based index for agricultural drought assessment: SMADI**
 418 **application in Pernambuco State-Brazil**, Remote Sensing of Environment 252 (2021) 112124. [doi:10.1016/j.rse.2020.112124](https://doi.org/10.1016/j.rse.2020.112124).
 419 URL <https://linkinghub.elsevier.com/retrieve/pii/S0034425720304971>
- 420 [41] F. N. Kogan, Application of vegetation index and brightness temperature for drought detection, Advances in Space
 421 Research 15 (11) (1995) 91–100. [doi:10.1016/0273-1177\(95\)00079-T](https://doi.org/10.1016/0273-1177(95)00079-T)
- 422 [42] A. Cui, J. Li, Q. Zhou, R. Zhu, H. Liu, G. Wu, Q. Li, **Use of a multiscale GRACE-based standardized terrestrial water**
 423 **storage index for assessing global hydrological droughts**, Journal of Hydrology 603 (2021) 126871. [doi:10.1016/j.jhydrol.2021.126871](https://doi.org/10.1016/j.jhydrol.2021.126871).
 424 URL <https://linkinghub.elsevier.com/retrieve/pii/S0022169421009215>
- 425 [43] P. Aceituno, J. P. Boisier, R. Garreaud, R. Rondanelli, J. A. Rutllant, **Climate and Weather in Chile**, in: B. Fernández,
 426 J. Gironás (Eds.), Water Resources of Chile, Vol. 8, Springer International Publishing, Cham, 2021, pp. 7–29.
 427 URL https://link.springer.com/10.1007/978-3-030-56901-3_2
- 428 [44] R. D. Garreaud, **The Andes climate and weather**, Advances in Geosciences 22 (2009) 3–11. [doi:10.5194/adgeo-22-3-2009](https://doi.org/10.5194/adgeo-22-3-2009).
 429 URL <https://adgeo.copernicus.org/articles/22/3/2009/>
- 430 [45] H. E. Beck, T. R. McVicar, N. Vergopolan, A. Berg, N. J. Lutsko, A. Dufour, Z. Zeng, X. Jiang, A. I. J. M. van Dijk, D. G.
 431 Miralles, **High-resolution (1 km) Köppen-Geiger maps for 1901–2099 based on constrained CMIP6 projections**, Scientific
 432 Data 10 (1) (Oct. 2023). [doi:10.1038/s41597-023-02549-6](https://doi.org/10.1038/s41597-023-02549-6).
 433 URL <https://dx.doi.org/10.1038/s41597-023-02549-6>
- 434 [46] R Core Team, **R: A Language and Environment for Statistical Computing**, R Foundation for Statistical Computing,
 435 Vienna, Austria, 2023.
 436 URL <https://www.R-project.org/>
- 437 [47] K. Hufkens, R. Stauffer, E. Campitelli, **The ecwmf package: an interface to ECMWF API endpoints** (2019).
 438 URL <https://bluegreen-labs.github.io/ecmwfr/>
- 439 [48] R. J. Hijmans, **terra: Spatial Data Analysis**, 2023.
 440 URL <https://CRAN.R-project.org/package=terra>
- 441 [49] E. Pebesma, R. Bivand, **Spatial Data Science: With applications in R**, Chapman and Hall/CRC, London, 2023.
 442 URL <https://r-spatial.org/book/>
- 443 [50] E. Pebesma, **Simple Features for R: Standardized Support for Spatial Vector Data**, The R Journal 10 (1) (2018) 439–446.
 444 [doi:10.32614/RJ-2018-009](https://doi.org/10.32614/RJ-2018-009).
 445 URL <https://doi.org/10.32614/RJ-2018-009>
- 446 [51] S. Beguería, S. M. Vicente-Serrano, **SPEI: Calculation of the Standardized Precipitation-Evapotranspiration Index**, 2023.
 447 URL <https://CRAN.R-project.org/package=SPEI>
- 448 [52] K. Didan, MOD13Q1 MODIS/Terra Vegetation Indices 16-Day L3 Global 250m SIN Grid V006, Tech. rep., NASA EOSDIS
 449 Land Processes DAAC (2015). [doi:https://dx.doi.org/10.5067/MODIS/MOD13Q1.006](https://dx.doi.org/10.5067/MODIS/MOD13Q1.006)
- 450 [53] G. H. Hargreaves, **Defining and Using Reference Evapotranspiration**, Journal of Irrigation and Drainage Engineering
 451 120 (6) (1994) 1132–1139. [doi:10.1061/\(ASCE\)0733-9437\(1994\)120:6\(1132\)](https://doi.org/10.1061/(ASCE)0733-9437(1994)120:6(1132)).
 452 URL <https://ascelibrary.org/doi/10.1061/%28ASCE%290733-9437%281994%29120%3A6%281132%29>
- 453 [54] Z. Hao, A. AghaKouchak, **Multivariate Standardized Drought Index: A parametric multi-index model**, Advances in Water
 454 Resources 57 (2013) 12–18. [doi:10.1016/j.advwatres.2013.03.009](https://doi.org/10.1016/j.advwatres.2013.03.009).
 455 URL <https://linkinghub.elsevier.com/retrieve/pii/S0309170813000493>
- 456 [55] A. AghaKouchak, **A baseline probabilistic drought forecasting framework using standardized soil moisture index: applica-**
 457 **tion to the 2012 United States drought**, Hydrology and Earth System Sciences 18 (7) (2014) 2485–2492. [doi:10.5194/hess-18-2485-2014](https://doi.org/10.5194/hess-18-2485-2014).
 458 URL <https://hess.copernicus.org/articles/18/2485/2014/>
- 459 [56] R. D. Garreaud, J. P. Boisier, R. Rondanelli, A. Montecinos, H. H. Sepúlveda, D. Veloso-Aguila, **The Central Chile**
 460 **Mega Drought (2010–2018): A climate dynamics perspective**, International Journal of Climatology 40 (1) (2020) 421–439.
 461 [doi:10.1002/joc.6219](https://doi.org/10.1002/joc.6219).
 462 URL <https://rmets.onlinelibrary.wiley.com/doi/10.1002/joc.6219>

- 466 [57] M. Abramowitz, I. A. Stegun, Handbook of mathematical functions with formulas, graphs, and mathematical tables, Vol. 55, US Government printing office, 1968.
- 467 [58] D. S. Wilks, Empirical distributions and exploratory data analysis, Statistical Methods in the Atmospheric Sciences 100 (2011).
- 468 [59] Y. Zhao, D. Feng, L. Yu, X. Wang, Y. Chen, Y. Bai, H. J. Hernández, M. Galleguillos, C. Estades, G. S. Biging, J. D. Radke, P. Gong, [Detailed dynamic land cover mapping of Chile: Accuracy improvement by integrating multi-temporal data](#), Remote Sensing of Environment 183 (2016) 170–185. doi:[10.1016/j.rse.2016.05.016](https://doi.org/10.1016/j.rse.2016.05.016).
URL <https://linkinghub.elsevier.com/retrieve/pii/S0034425716302188>
- 469 [60] P. K. Sen, [Estimates of the Regression Coefficient Based on Kendall's Tau](#), Journal of the American Statistical Association 63 (324) (1968) 1379–1389. doi:[10.1080/01621459.1968.10480934](https://doi.org/10.1080/01621459.1968.10480934).
URL <http://www.tandfonline.com/doi/abs/10.1080/01621459.1968.10480934>
- 470 [61] M. Kendall, Rank correlation methods (4th ed, 2d impression). Griffin, 1975.
- 471 [62] R. Tibshirani, J. Bien, J. Friedman, T. Hastie, N. Simon, J. Taylor, R. J. Tibshirani, [Strong rules for discarding predictors in lasso-type problems](#) (Nov. 2010).
URL <http://arxiv.org/abs/1011.2234>
- 472 [63] A. E. Hoerl, R. W. Kennard, [Ridge Regression: Biased Estimation for Nonorthogonal Problems](#), Technometrics 12 (1) (1970) 55–67. doi:[10.1080/00401706.1970.10488634](https://doi.org/10.1080/00401706.1970.10488634).
URL <http://www.tandfonline.com/doi/abs/10.1080/00401706.1970.10488634>
- 473 [64] T. K. Ho, Random decision forests, in: Proceedings of 3rd international conference on document analysis and recognition, Vol. 1, IEEE, 1995, pp. 278–282.
- 474 [65] S. M. Vicente-Serrano, D. Peña-Angulo, S. Beguería, F. Domínguez-Castro, M. Tomás-Burguera, I. Noguera, L. Gimeno-Sotelo, A. El Kenawy, [Global drought trends and future projections](#), Philosophical Transactions of the Royal Society A: Mathematical, Physical and Engineering Sciences 380 (2238) (2022) 20210285. doi:[10.1098/rsta.2021.0285](https://doi.org/10.1098/rsta.2021.0285).
URL <https://royalsocietypublishing.org/doi/10.1098/rsta.2021.0285>
- 475 [66] S. M. Vicente-Serrano, D. G. Miralles, F. Domínguez-Castro, C. Azorin-Molina, A. El Kenawy, T. R. McVicar, M. Tomás-Burguera, S. Beguería, M. Maneta, M. Peña-Gallardo, [Global Assessment of the Standardized Evapotranspiration Deficit Index \(SEDI\) for Drought Analysis and Monitoring](#), Journal of Climate 31 (14) (2018) 5371–5393. doi:[10.1175/JCLI-D-17-0775.1](https://doi.org/10.1175/JCLI-D-17-0775.1).
URL <https://journals.ametsoc.org/doi/10.1175/JCLI-D-17-0775.1>
- 476 [67] M. Meroni, F. Rembold, D. Fasbender, A. Vrieling, [Evaluation of the Standardized Precipitation Index as an early predictor of seasonal vegetation production anomalies in the Sahel](#), Remote Sensing Letters 8 (4) (2017) 301–310. doi:[10.1080/2150704X.2016.1264020](https://doi.org/10.1080/2150704X.2016.1264020).
URL <https://www.tandfonline.com/doi/full/10.1080/2150704X.2016.1264020>
- 477 [68] A. Miranda, A. D. Syphard, M. Berdugo, J. Carrasco, S. Gómez-González, J. F. Ovalle, C. A. Delpiano, S. Vargas, F. A. Squeo, M. D. Miranda, C. Dobbs, R. Mentler, A. Lara, R. Garreaud, [Widespread synchronous decline of Mediterranean-type forest driven by accelerated aridity](#), Nature Plants 9 (11) (2023) 1810–1817. doi:[10.1038/s41477-023-01541-7](https://doi.org/10.1038/s41477-023-01541-7).
URL <https://www.nature.com/articles/s41477-023-01541-7>